CHINESE JOURNAL OF GEOPHYSICS Vol.49, No.6, 2006, pp: 1665∼1675

AVO NUMERICAL SIMULATION OF GAS HYDRATE REFLECTORS BENEATH SEAFLOOR

RUAN Ai-Guo LI Jia-Biao CHU Feng-You LI Xiang-Yun

Second Institute of Oceanography & Key Lab of Submarine Geosciences, State Oceanic Administration, Hangzhou 310012*, China*

Abstract The AVO numerical method is used to 6 models of layered gas hydrate systems beneath seafloor, composed of methane hydrate bearing sediment, free gas bearing sediment and saturated sediment, to simulate the formation mechanism of BSR, double BSR and the vertical distribution of the gas hydrate system to make theoretical explanation of some practical problems. The main conclusions are as follows: (1) The presence of evident ocean bottom simulating reflector (BSR) is closely related to the existence of free gas and the seismic profile "BSR" maybe is not uniquely linked with methane hydrate but only shows the existence of gas. Inversely, methane hydrate may exists at the place without obvious BSR. (2) Free gas is possible to exist on the top of methane hydrate and forms a positive BSR above the normal BSR (BSR_1). (3) There are two possible elastic mechanisms for double BSR_0 under normal BSR_1. If the methane gas meets some obstruct layer on the path of upward migration or different gas components naturally are stratified, the vertical gradient distribution of methane gas would be formed with upper part saturation higher than lower part resulting in a negative reflector. On the other hand, if some residual hydrate exists in the free gas layer under methane hydrate, some kind of BSR with certain amplitude would occur. But for this case the polarity of BSR_0 maybe is difficult to be discriminated, depending on the gas saturation above or beneath the residual hydrate and the thickness of residual hydrate.

Key words Natural gas hydrates, Layering interface, BSR, AVO, Numerical simulation

1 INTRODUCTION

Marine gas hydrates are recognized as a potential future energy resource and economically important[1,2], their trapped methane gas, a kind of greenhouse gas, may have a major impact on the global climate system[3∼6], and gas hydrates and free gas may play an important role in marine geo-hazards[7∼11]. Ocean bottom simulating reflectors (BSRs) that are broadly parallel to the seafloor with strong amplitude and negative polarity in seismic reflection profiles are associated with the base of gas hydrates stability zones and are the prominent indicators of the presence of gas hydrates[12∼18]. There are mainly two viewpoints and correspondingly two models for BSR, the "hydrate wedge model"[19,20] suggests that BSR is the interface between gas hydrate bearing sediment and water saturated sediment and the upper gas hydrate is emphasized but free gas may be absent, while the "free gas zone model"[20] suggests that BSR is the interface between gas hydrate bearing sediment and free gas bearing sediment and the lower free gas is emphasized. Both seismic waveform inversion of practical data and ODP drilling have shown that BSRs of large amplitude are associated with free methane gas[17,21∼24].

At present the knowledge of the vertical distribution of gas hydrates above BSR is not enough. Researches on several continental margins indicate that gas hydrates are increasingly distributed with depth[25]. The discovery of double BSRs promotes the understandings of detailed structure of the gas hydrates system[26∼30] in addition to BSR that is even believed to be caused by the whole layer containing free gas[31]. The practical existence zone of hydrate begins to be distinguished from the hydrate stability zone based on phases balance curves[32]. It is believed that the top and bottom of these zones maybe are not coincident, the latter is larger. The top of free gas may be coincident neither with the bottom of hydrate existence zone nor with the bottom of hydrate stability zone and there exist some zones without free gas or hydrate either. Such viewpoints have been used to interpret practical observed data successfully. In the Storegga Slide area western Norway

E-mail: Ruan@sio.hzcnc.net

double BSRs were discovered[11,27,28,33~35], in addition to the negatively polarized normal BSR_1 associated with the bottom of hydrate, above which there exists a positively polarized abnormal bottom simulating reflector, named BSR_2 corresponding to the top of hydrate, above which a low velocity zone corresponding to gas clearly exists. Moreover, there is another reflector 45m beneath BSR_1, called BSR_0, which is also positively polarized corresponding to the top of free gas. However one question is raised here. It is easy to understand the observed positive polarity of BSR_2, for it is the bottom of low velocity layer formed by free gas. But the observed positive polarity of BSR_0 is contrary to the theoretical expectation of negative polarity of reflected wave, for the medium above BSR_0 is associated with saturated sediment or pale-hydrate of higher velocity while the medium beneath BSR_0 is free gas of lower velocity. The given explanation for this question is that the observed positive polarity of BSR_0 is due to the mutual interference of reflected waves from the top and bottom interfaces of the low velocity zone containing free gas[28]. There are two explanations of formation mechanisms for BSR_0. One is the residual bottom of pale-hydrate because of upwards migration of hydrate due to temperature and pressure changes. The other is a kind of compound gases between BSR_1 and BSR_0. Double BSRs were also discovered in the southeastern trough of the Japan Sea[26,30,36,37], where the negatively polarized BSR_1 is the normal bottom simulating reflector corresponding to the bottom of gas hydrates zone and the reflector with negative polarity 50m under BSR_1 is another BSR, named BSR_2, beneath which is low velocity free gas layer. It is believed that the low velocity layer between BSR_1 and BSR_2 is water saturated sediment without gas hydrates or containing little gas. Obviously the double BSRs in the above two areas are some different with each other. Furthermore, some drilling results have raised doubts on the uniqueness of the relation between BSR and gas hydrates. It is known that the drilling on the continental margins of South and North America did not reveal an adequate volume of gas hydrates and gas in the area of BSR[38]. Contrarily, the drilling of ODP Leg 127 in the northeastern Japan Sea, ODP Leg 112 in the continental margin of Peru and DSDP Leg 84 in mid-American Trench found gas hydrate in the areas without BSR presence[39], and also in the Blake Ridge ODP Leg 164 discovered gas hydrates and free gas in the areas without evident BSR[17].

The facts mentioned above show that using a single interface BSR to separate gas hydrate and free gas makes the understanding of gas hydrates system be too simplified. Localized factors such as geological structure, deposition process, carbon content, gas hydrate content and free gas content have great influences on BSR. The gas hydrate bearing sediment is not a uniform layer and may consist of sub-layers or gradient layers. Above the top of a gas hydrate layer there may be methane gas and beneath a gas hydrate bottom there may be some complicated layering cases in the free gas zone. All of these cases are worth to be studied carefully. The methods usually used for the study of the layering structure of the gas hydrate system are AVO simulation[40~43] and full wave inversion[23,30,44~47]. For discussion of the elastic mechanisms of BSR and double BSRs and theoretical interpretation or confirmation of some observed phenomena, in this paper AVO simulation method is used to the gas hydrates system to demonstrate the reflecting features of various fine structures and to clarify their elastic parameter conditions.

2 AVO SIMULATION METHOD

Usually in AVO analysis some corrections such as spreading correction, absorption compensation, effects of thin layers, topography and scattering should be conducted in practical seismic data processing. But for numerical simulation it is supposed that these corrections have been finished or unnecessary, interfaces are horizontal, wave amplitude is only associated with interface reflecting coefficient and amplitude versus offset uniquely determined by the elastic parameters of the interface. It should be pointed out that the formula for the calculation of the reflection coefficient in AVO is an approximate expression on the condition that the jump of properties on two sides of an interface is small but without a quantitative indicator[48]. Fortunately, in our previous research it has been confirmed that this approximate formula is suitable for gas hydrate systems and its error is acceptable[49]. Since the condition for the substitution of root mean square velocity for layer velocity is a small offset range, the case of the incident angle larger than the critical angle is not considered in the AVO

simulation in this paper.

2.1 Calculation of Reflection Coefficients

The first-order approximate Zoeppritz's equation for P wave incidence and reflection is[48]

$$R_{\rm PP} = \frac{1}{2}(1-4\beta^2p^2)\frac{\Delta\rho}{\rho} + \frac{1}{2\cos^2 i}\frac{\Delta\alpha}{\alpha} - 4\beta^2p^2\frac{\Delta\beta}{\beta}, \tag{1}$$

with

$$\begin{cases} \Delta\rho = \rho_2 - \rho_1, \quad \Delta\alpha = \alpha_2 - \alpha_1, \quad \Delta\beta = \beta_2 - \beta_1 \\ \rho = \dfrac{1}{2}(\rho_2+\rho_1), \quad \alpha = \dfrac{1}{2}(\alpha_2+\alpha_1), \quad \beta = \dfrac{1}{2}(\beta_2+\beta_1), \quad i = \dfrac{1}{2}(i_2+i_1), \end{cases} \tag{2}$$

where α, β and ρ are P wave velocity, S wave velocity and density, respectively, subscripts 1 and 2 denote the up side and down side of an interface, respectively and p is the horizontal slowness.

2.2 Calculation of Travel Time and Incident Angle of Reflected Waves

For multi-layered media on the condition of small offset, one reflection layer together with the layers above it can be expressed as a uniform layer, of which the velocity is the root mean square velocity of these layers. Suppose the seismic source and geophones are horizontally arranged along X axis on the surface of the sea and there are N geophones and K layers, the P wave travel time for reflecting interface k and geophone n can be written as

$$t^2(k,n) = t_0^2(k) + \frac{x^2(n)}{\alpha_{\rm rms}^2(k)}, \tag{3}$$

with

$$\begin{cases} t_0(k) = 2\sum\limits_{i=1}^{k} t_i = 2\sum\limits_{i=1}^{k}\dfrac{h_i}{\alpha_i}, \\ \alpha_{\rm rms}(k) = \left[\sum\limits_{i=1}^{k} t_i\alpha_i^2 \Big/ \sum\limits_{i=1}^{k} t_i\right]^{\frac{1}{2}} = \left[\sum\limits_{i=1}^{k}\alpha_i h_i \Big/ \sum\limits_{i=1}^{k}\dfrac{h_i}{\alpha_i}\right]^{\frac{1}{2}}, \end{cases} \tag{4}$$

where $t_0(k)$ is the double travel time at zero offset for interface k, $\alpha_{\rm rms}(k)$ is the root mean square velocity of layer k and its above layers, α_i and h_i are single layer velocity and thickness, respectively, and $x(n)$ is the offset of geophone n.

From Snell's law the incident angle of reflector k for geophone n is

$$\sin i(k,n) = [x(n)\alpha(k)]/[\alpha_{\rm rms}^2(k)t(k,n)]. \tag{5}$$

2.3 Synthetic Seismogram of AVO

For interesting interfaces the incident angle and travel time are calculated by Eqs.(3)∼(5), ray parameter and transmission angle are calculated by using Snell's law, then approximate incident angle is obtained based on Eq.(2). Finally the reflection coefficients in Eq.(1) are multiplied by the wavelet of the source to form the AVO wave records at all geophones. Since only fewer reflectors such as sea bottom and BSRs are interested, it is unnecessary to calculate the reflected waves from every interface such as subsurfaces in a homogeneous layer. The Ricker wavelet is chosen as the seismic source used in the simulation with dominant frequency 40Hz. The total wave recorded length is 4s with sampling rate 0.002s.The number of geophones is 100 with interval 200m.

3 MODELS AND PARAMETERS

In simulation the parameters of water saturated sediment, gas hydrate and free methane gas and the calculation method for layering velocity and density are chosen from the paper of Ecker et al.[24], the calculated parameters used in simulation are shown in Table 1. In gas hydrate model A gas hydrate is treated as fluid and in model B it is treated as solid mineral bone, their results are the upper and lower limitations of all models.

The porosity is supposed to be 50% for each model and the saturations of free gas and gas hydrate are chosen in a popular range[46] and indicated in each model. Except the first layer of sea water 1500m thick from surface to seafloor, the others are divided into several sub-layers depending on the thickness of the layer. In this paper totally six models or cases are considered:

(1) Sea water (1500m)→saturated sediment (200m)→gas hydrate (400m, 20%) (BSR)→saturated sediment (200m). The feature of this model is no free gas and both sides of gas hydrate are water saturated sediments.

(2) Sea water (1500m)→saturated sediment (300m) (BSR)→free gas (400m,5%). The feature of this model is that no gas hydrate and only free gas exists.

(3) Sea water (1500m)→saturated sediment (200m)→gas hydrate (400m,20%) (BSR)→free gas (300m,5%). The BSR in this model consists of gas hydrate and free gas.

(4) Sea water (1500m)→saturated sediment (200m)→gradient layers of gas hydrate (500m: 1%∼5%∼10%∼15%∼20%) (BSR)→gradient layers of free gas (200m: 2%∼4%). In this model the saturations of gas hydrate and free gas increase with depth.

(5) Sea water (1500m)→saturated sediment(160m)→free gas (160m: 2%) (BSR_2)→gas hydrate (200m: 20%) (BSR_1)→free gas (50m: 2%)→gas hydrate (50m: 10%) (BSR_0)→free gas (50m: 1%). In this model several BSRs with different mechanisms are designed.

(6) Sea water (1500m)→free gas (160m: 2%) (BSR_2)→gas hydrate (300m: 20%) (BSR_1)→gradient layers of gas hydrate (60m: 15%∼10%) (BSR_0)→free gas (60m: 2%). In this model several BSRs with different mechanisms are designed too.

Table 1 Main parameters of models

	Saturation $S/(\%)$	P wave $V_P/(km\cdot s^{-1})$	S wave $V_S/(km\cdot s^{-1})$	Density $\rho/(kg\cdot cm^{-3})$
Saturated sediment	100	1.7516	0.5162	1.831
Methane gas bearing sediment	5	1.3298	0.5191	1.811
	4	1.3801	0.5185	1.815
	2	1.5184	0.5173	1.823
	1	1.6176	0.5168	1.827
Gas hydrate bearing sediment, model A	20	1.8386	0.5181	1.818
	15	1.8154	0.5176	1.821
	10	1.7933	0.5172	1.824
	5	1.7720	0.5167	1.828
	1	1.7556	0.5163	1.830
Gas hydrate bearing sediment, model B	20	1.9261	0.5528	1.713
	15	1.8794	0.5393	1.734
	10	1.8347	0.5281	1.760
	5	1.7919	0.5198	1.791
	1	1.7594	0.5164	1.822

4 SIMULATING RESULTS AND DISCUSSION

4.1 Model 1

The designed BSR of this model is due to the property jump from gas hydrate bearing sediment to sea water saturated sediment. The synthetic seismogram, amplified wave forms and AVO curves for hydrate model A shown in Fig. 1 indicate that when BSR consists of gas hydrate bearing sediment (20%) and water saturated sediment, in comparison with the reflection of seafloor, it is of negative polarity and weak amplitude about 10% less of seafloor's, which suggests that the existence of gas hydrate can not cause great change of reflectivity[21,22] and gas hydrate may exist in the place without obvious BSR. The AVO effects of seafloor and BSR are negative and positive, respectively but both are small. The results shown in Fig. 2 are the same

modeling but using hydrate model B. Except for a very fine difference in the reflection coefficient, nearly no difference exists between the two hydrate models showing that the change of the hydrate model has no effect on simulation.

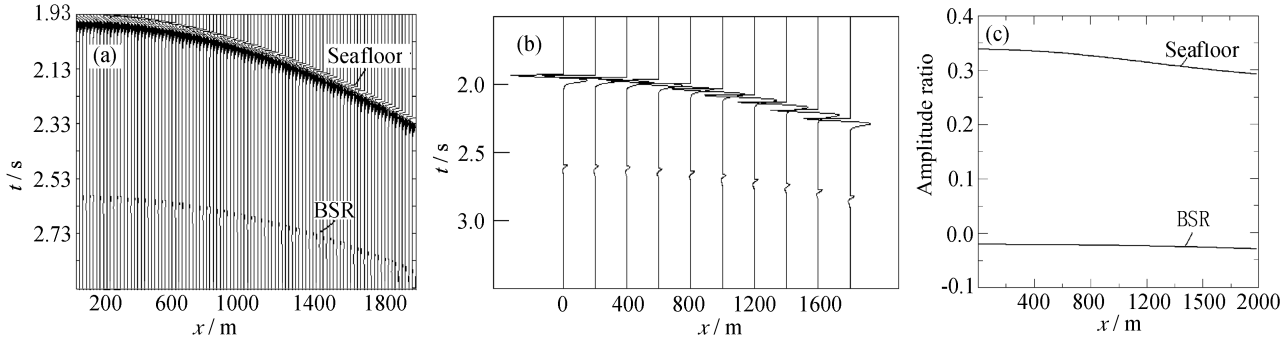

Fig. 1 Model 1 (gas hydrate model A)

x is the offset, t is the two-way time. (a) Synthetic seismogram; (b) Amplified waveform; (c) AVO curves.

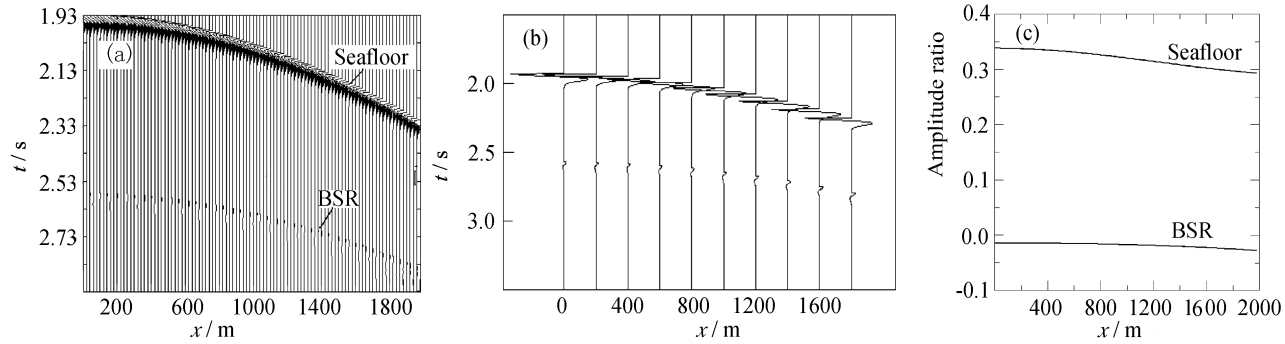

Fig. 2 Model 1 (gas hydrate model B)

(a) Synthetic seismogram; (b) Amplified waveform; (c) AVO curves.

4.2 Model 2

The designed BSR of this model is due to the property jump from sea water saturated sediment to free methane gas bearing sediment (5%). The synthetic seismogram, amplified wave forms and AVO curves of this modeling are shown in Fig. 3. It can be seen that in comparison with the reflection of seafloor this BSR is of negative polarity and obvious amplitude, 50% less of seafloor's at zero offset and 50% more of seafloor's at larger offset. It suggests that the existence of free gas plays an important role in reflectivity[21,22]. "BSR" maybe only indicates methane gas rather than hydrate and the AVO method is suitable for gas hydrates seismic research.

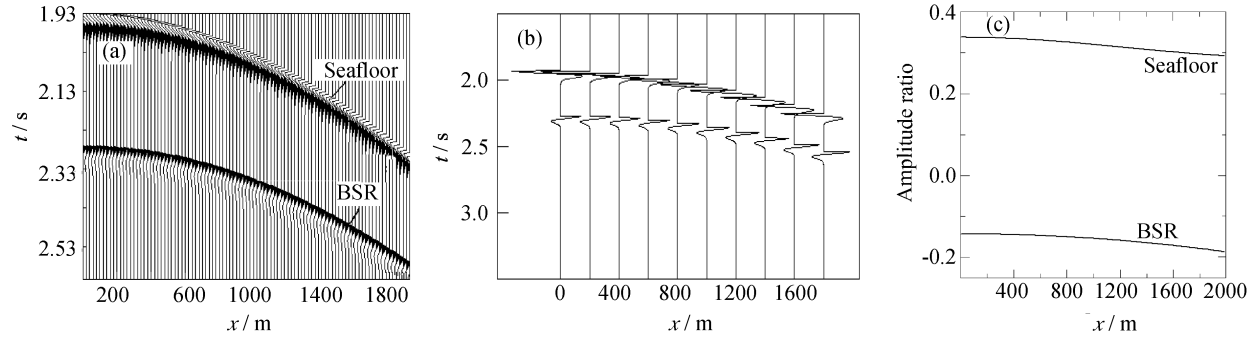

Fig. 3 Model 2

(a) Synthetic seismogram; (b) Amplified waveform; (c) AVO curves.

4.3 Model 3

The designed BSR of this model is a popular one that is due to the property jump from gas hydrate (20%) to free gas (5%). The simulated results using gas hydrate model A in Fig. 4 show that in comparison with the reflection of seafloor, the polarity BSR is of negative and the amplitude is obvious, 50% of seafloor's at zero offset and 70% of seafloor's at larger offset. In comparison with model 1, it also suggests that the existence of free gas plays an important role in BSR amplitude. Fig. 5 shows the results of the same modeling but using hydrate model B and has little different from Fig. 4.

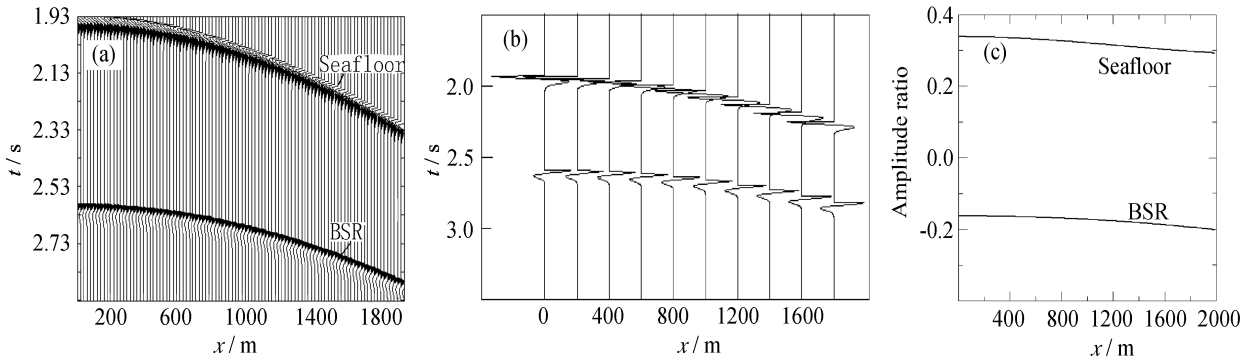

Fig. 4 Model 3 (gas hydrate model A)

(a) Synthetic seismogram; (b) Amplified waveform; (c) AVO curves.

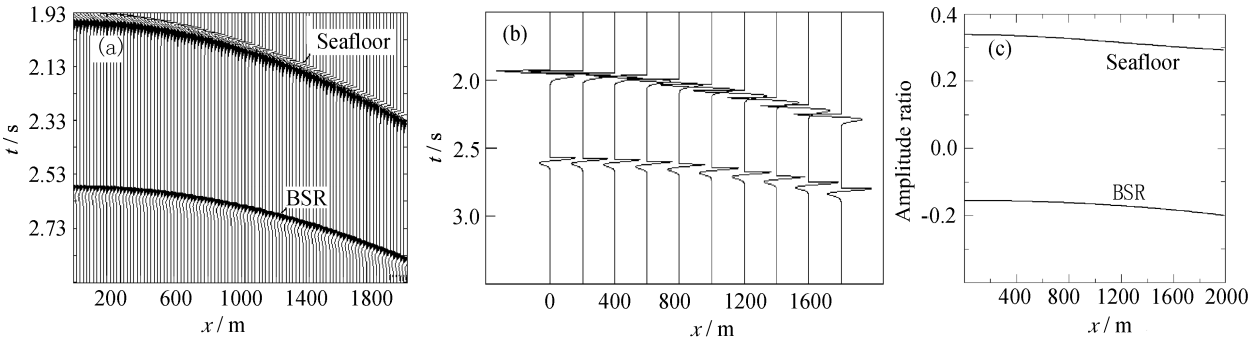

Fig. 5 Model 3 (gas hydrate model B)

(a) Synthetic seismogram; (b) Amplified waveform; (c) AVO curves.

Some conclusions can be reached based on the comparisons of these three models and the parameters listed in Table 1. (1) The condition for negative polarity reflection is only that the velocity over BSR is larger than the velocity beneath BSR and density has no obvious impact and the density over BSR could be smaller than the density beneath BSR. (2) The existence of free gas plays an important role in large amplitude of BSR, contrarily, gas hydrate can not greatly increase reflectivity, which implies that the BSR is mainly due to free gas. In model 2 the simulated obvious "BSR" without gas hydrate can still be called BSR. This modeling only shows a possibility or explanation for "BSR" without association with gas hydrate and in practice whether a negative reflector can be called BSR or not also depends on other characteristics such as parallel to seafloor and obliquely cutting deposition layers. (3) The AVO effect of BSR is obvious and the reflection amplitude increases with offset. But the change of gas hydrate model has no obvious influence on simulated results, therefore in following modeling for gas hydrate only model B is used.

4.4 Model 4

In this model a gas hydrates zone is over BSR and a free gas zone is underlying BSR and in both zones the saturations of gas hydrate or free gas are downward increasing in gradient. Fig. 6 shows that in the gas hydrate

zone there are some very weak positively polarized reflectors due to gradient changes of saturation that causes downward increasing in velocity and decreasing in density. The BSR between the gas hydrate zone and free gas zone is of negative polarity and obvious amplitude, 25% of seafloor's at zero offset and 60% of seafloor's at larger offset. In the free gas zone both the velocity of P wave and density are downward decreasing (velocity of S wave is increasing faintly). Another BSR (named double BSR_0) with negative polarity on the gradient interface is formed and its amplitude is relatively obvious, about 50% of normal BSR, which suggests that the subdivision of the free gas zone can result in double BSRs. From the viewpoint of reflection polarity only, this simulated result is consistent with the case in the southeastern trough of the Japan Sea but contrary to the case in the Storegga Slide area of western Norway[34]. The implication of this modeling is that if the methane gas met some obstruct layer on the path of upward migration or different gas components were naturally stratified, subdivision of free gas was formed that would cause double BSRs, even the top of free gas zone was coincident with BSR.

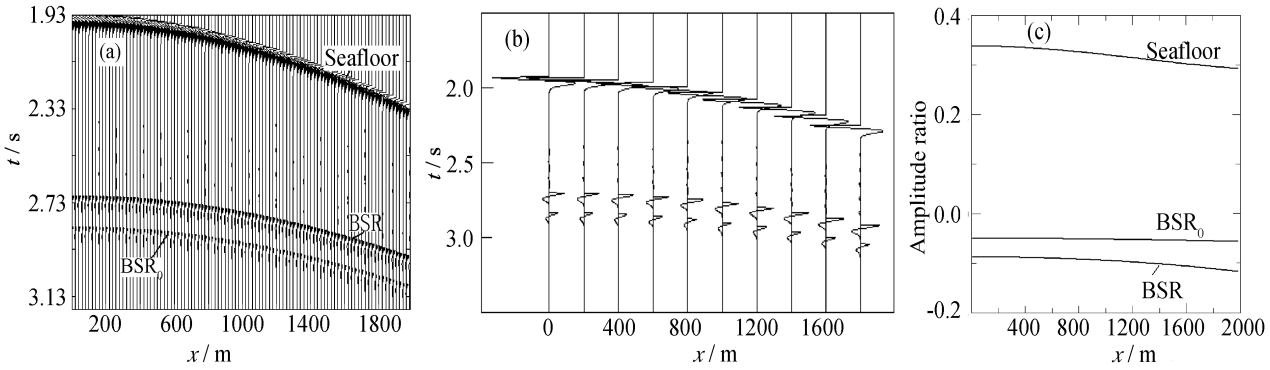

Fig. 6 Model 4 (gas hydrate model B)

(a) Synthetic seismogram; (b) Amplified waveform; (c) AVO curves.

4.5 Model 5

For simulating double BSRs, in this model three kinds of BSR are designed from upper to lower, BSR_2 a layer containing free gas (2%) covers a layer containing gas hydrate (20%), BSR_1 (normal BSR) the layer containing gas hydrate (20%) covers another layer containing free gas (2%) and BSR_0 free gas bearing sediment (1%) is covered by a pale-hydrate layer (10%). The simulated results of this model shown in Fig. 7 can be summarized as follows. (1) The occurrence of a free gas layer on the top of gas hydrate could produce a positive reflector (BSR_2) with amplitude 30% of seafloor's similar to the case in the Storegga Slide area of western Norway[34,35] and on the top of free gas covered by a water saturated sediment zone a negative reflecting is produced, but no such phenomenon has been reported in practice. It suggests that free gas may exist on the top of gas hydrate but this gas zone should be homogeneously distributed in vertical direction without other interfaces in it. (2) The large amplitude (30% of seafloor) of negative reflection (BSR_1) is associated with free gas beneath gas hydrate that is called normal BSR. If there is a residual hydrate layer in the free gas zone beneath hydrate, on the top of residual hydrate the reflection is positive with amplitude 30% of seafloor's, simultaneously at the bottom of the residual hydrate the reflection is negative with amplitude 50% of BSR_1. Therefore, if the layer of residual hydrate is very thin, these two reflected waves with different polarity would be difficult to be discriminated. If we take the former as double BSRs (BSR_0) the simulated result is consistent with that of the Norwegian case but if we take the latter as double BSRs (BSR_2) the simulated result is consistent with that of the Japanese case. Maybe the polarity determination of such double BSR_0 depends on the saturation of free gases above and below the residual hydrate, higher saturation results in stronger amplitude.

For further clarification of the polarity problem of BSR_0 due to the thickness of residual hydrate, a supplemented calculation is made in which the thickness of the residual hydrate is reduced from 50m to 25m.The simulated amplified waveforms are shown in Fig. 7d. Obviously, the polarity of BSR_0 becomes more difficult to

be discriminated due to the more serious interfering between two reflected waves from the top and bottom of residual hydrate that is much thin. This numerical simulation maybe provides us a direct explanation for the viewpoint of Andreassen et al.[28] about the polarity of BSR_0.

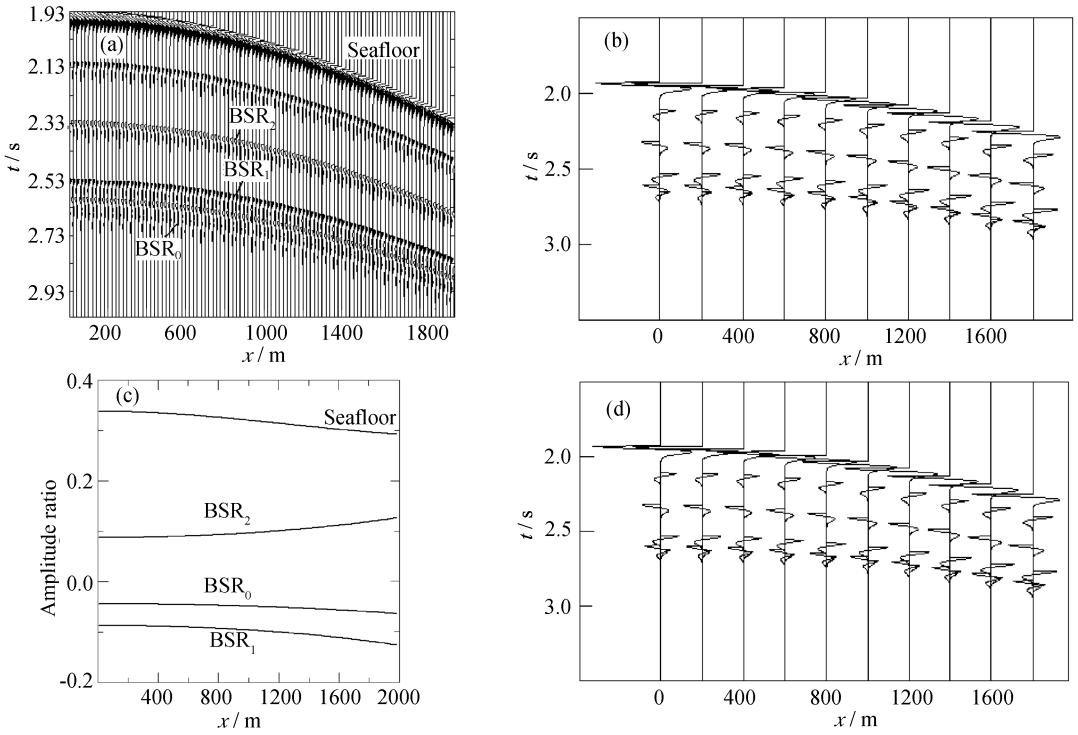

Fig. 7 Model 5 (gas hydrate model B)

(a) Synthetic seismogram; (b) Amplified waveform; (c) AVO curves; (d) Amplified waveform for modified model.

4.6 Model 6

In this model also three kinds of BSR are designed from upper to lower, BSR_2 a layer containing free gas (2%) covers a layer containing gas hydrate (20%), BSR_1 (normal BSR) the layer containing gas hydrate (20%) covers a gradient layer of gas hydrate (15%∼10%) and BSR_0 free gas zone (2%) is covered by the gas hydrate layer (10%). The simulated results of this model are shown in Fig. 8. This model is characterized by the small amplitude of BSR_1 that is far less than others, because here BSR_1 is caused by the property jump in the gradient zone of gas hydrate without free gas. This simulated result is contrary to practical observations, which means if pale-hydrate exists beneath gas hydrate there must be some gas between them, for large amplitude of

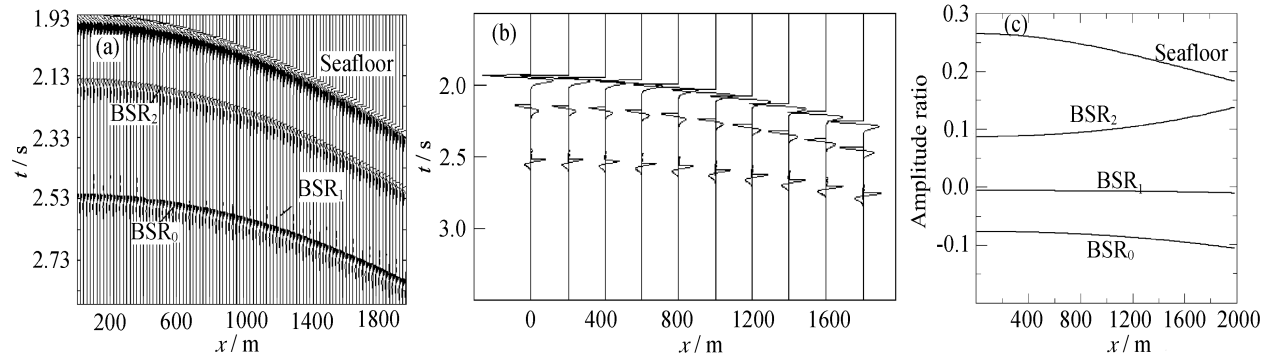

Fig. 8 Model 6 (gas hydrate model B)

(a) Synthetic seismogram; (b) Amplified waveform; (c) AVO curves.

BSR is closely associated with free gas. The result also shows that the amplitudes of double BSR_0 due to free gas and gas hydrate are relatively larger but the polarities depend on relative positions between free gas and gas hydrate.

5 CONCLUSIONS

The AVO numerical method is used to 6 models of layered gas hydrates systems to simulate seismic reflection characteristics of various reflectors beneath seafloor composed of methane hydrate bearing sediment, free gas bearing sediment and saturated sediment. The elastic conditions for the mechanism of BSR and double BSRs are studied and some practical problems are theoretically explained. The main conclusions are as follows:

(1) The presence of ocean bottom simulating reflector (BSR) is closely associated with free gas that is the absolute necessity for occurrence of strong reflection amplitude of BSR, indicating BSR is mainly due to the existence of free gas beneath seafloor. Whether the medium above free gas is methane hydrate bearing sediment or water saturated sediment has no obvious influence on the amplitude of BSR. Therefore the determination of BSR in seismic profiles should consider the existence of gap zones that reflect the occurrence of homogeneous and dense media, and whether the reflection is interface parallel to seafloor and other factors. Otherwise, "BSR" maybe is not uniquely linked with methane hydrate, the area without obvious BSR may has gas hydrate while the area of obvious "BSR" may not correspond to gas hydrate. The gas hydrate model A has similar results as model B.

(2) Free gas is possible to exist on the top of methane hydrate which could form a positive BSR above the normal BSR (BSR_1) and this low velocity layer should be continuously and homogeneously distributed without layering.

(3) There are two possible elastic mechanisms for BSR_0 under normal BSR_1. If the methane gas met some obstruct layer on the path of upward migration or different gas components were naturally stratified, the vertical gradient distribution of methane gas would be formed with gas saturation of the upper part higher than lower part and a negative reflector was formed. If some residual hydrate layer exists in the free gas zone under methane hydrate, some kinds of BSR with certain amplitude would occur. But in this case the polarity of BSR_0 maybe is difficult to be discriminated, depending on the gases saturations. In addition, a very thin layer of residual hydrate will also cause difficulty in the polarity discrimination of BSR_0.

ACKNOWLEDGMENTS

Dr. Song Hai-Bin of the Institute of Geology and Geophysics, Chinese Academy of Sciences read the manuscript and put forward some constructive suggestions. Most of the suggestions from anonymous reviewers are accepted by the authors, which greatly improved the present paper. This work was supported by the National Key Basic Research Project (G2000046704).

REFERENCES

[1] Kvenvolden K A. Methane hydrate-A major reservoir of Carbon in the shallow geosphere. *Chem. Geol.*, 1988, **71**: 41∼71

[2] MacDonald G J. The future of methane as an energy resource. *Annu. Rev. Energy*, 1990, **15**: 53∼83

[3] Kvenvolden K A. Methane hydrates and global climate. *Global Biogeochem Cycles*, 1988, **2**: 221∼229

[4] Nisbet E G. The end of the ice age. *Can. J. Earth. Sci.*, 1990, **27**: 148∼157

[5] Leggett J. The nature of the greenhouse threat in Global warming. The Greenpeace Report. New York: Oxford Univ. Press, 1990. 14∼43

[6] Paull C K, Ussler W III, Dillon W P. Is the extent of glaciation limited by the marine gas-hydrates? *Geophys. Res. Lett.*, 1991, **18**: 432∼434

[7] McIver R D. Role of naturally occurring gas hydrates in sediment transport. *Am. Assoc. Pet. Geol. Bull.*, 1982, **66**(6): 789∼792

[8] Kayen R E, Lee H J. Pleistocene slope instability of gas hydrate-laden sediment on the Beaufort Sea Margin. *Marine Geotechnology*, 1991, **10**: 125∼141

[9] Kvenvolden K A. A primer on the geological occurrence of gas hydrate. In: Henriet J P, Mienert J eds. Gas Hydrates: Relevance to World Margin Stability and Climatic Changes. Geological Society of London Special Publication, 1998, **137**: 9∼30

[10] Sultan N, Cochonat P, Foucher J P, et al. Effect of gas hydrate dissociation on seafloor slope stability. In: Locat J, Mienert J eds. Submarine Mass Movements and Their Consequences. Kluwer Academic Publishers, Dordreeht, 2003. 103∼111

[11] Mienert J, Vanneste M, Bunz S, et al. Ocean warming and gas hydrate stability on the mid-Norwegian margin at the Storegga Slide. *Marine and Petroleum Geology*, 2005, **22**: 233∼244

[12] Markl R G, Bryan G M, Ewing J I. Structure of the Blake-Bahama outer ridge. *J. Geophys. Res.*, 1970, **75**: 4539∼4555

[13] Stoll R D, Ewing J, Bryan G M. Anomalous wave velocities in sediments containing gas hydrates. *J. Geophys. Res.*, 1971, **76**: 2090∼2094

[14] Shipley T H, Houston M H, Buller R T. Seismic evidence for wide-spread possible gas hydrate horizons on continental slopes and margins. *Am. Assoc. Pet. Geol. Bull.*, 1979, **63**: 2204∼2213

[15] Lodolo E, Camerlenghi A, Brancolini G. A bottom simulating reflector on the South Shetland Margin, Antarctic Peninsula. *Antarctic Sci.*, 1993, **5**: 207∼210

[16] Andreassen K, Hart P, Grantz A. Seismic studies of a bottom simulating reflector related to gas hydrate beneath the continental margin of the Beaufort Sea. *J. Geophys. Res.*, 1995, **100**: 12659∼12673

[17] Holbrook W S, Hoskins H, Wood W T, et al. Methane hydrate and free gas on the Blake Ridge from vertical seismic profiling. *Science*, 1996, **273**: 1840∼1843

[18] Kvenvolden K A, Lorenson T D. The global occurrence of natural gas hydrates. In: Paull C K, Dillon W P eds. Natural Gas Hydrates: Occurrence, Distribution and Detection. American Geophysical Union, Geophysical Monographs, 2001, **124**: 3∼18

[19] Hyndman R D, Davis E E. A mechanism for the formation of methane hydrate and seafloor bottom simulating reflectors by vertical fluid expulsion. *J. Geophys. Res.*, 1992, **97**: 7025∼7041

[20] Katzman R, Holbrook W S, Paull C K. Combined vertical-incident and wide-angle seismic study of a gas hydrate zone, Blake Ridge. *J. Geophys. Res.*, 1994, **99**: 17975∼17995

[21] Singh S C, Minshull T A, Spence G D. Velocity structure of a gas hydrate reflector. *Science*, 1993, **260**: 204∼207

[22] Mackay M E, Jarrard R D, Westbrook G K, et al. Origin of bottom-simulating reflectors: Geophysical evidence from the Cascadia accretionary prism. *Geology*, 1994, **22**: 459∼462

[23] Korenaga J, Holbrook W S, Singh S C, et al. Natural gas hydrates on the Southeast U.S. margin: Constraints from full waverform and travel time inversions of wide-angle seismic data. *J. Geophys. Res.*, 1997, **102**: 15345∼15365

[24] Ecker C, Dvorkin J, Nur A M. Estimating the amount of gas hydrate and free gas from marine seismic data. *Geophysics*, 2000, **65**(2): 565∼573

[25] Wood W T, Stoffa P L, Shipley T H. Quantitative detection of methane hydrate through high-resolution seismic velocity analysis. *J. Geophys. Res.*, 1994, **99**: 9681∼9695

[26] Ashi J, Tokuyama H. Cold seepage and gas hydrate BSR in Nankai Trough. Proc. of Inter. Workshop on Gas Hydrate Studies: The Second Joint Japan-Canada Workshop, 1997. 256∼273

[27] Posewang J, Miener J. The enigma of double BSRs: Indicators for changes in the hydrate stability field. *Geo-Marine Lett.*, 1999, **19**: 157∼163

[28] Andreassen K, Miener J, Bryn P, et al. A double gas- hydrate related bottom simulating reflector at the Norwegian continental margin. The Annals of the New York Acad. of Sci., 2000, **912**: 126∼135

[29] Song H, Matsubayashi O, Kuramoto S. Velocity structure of a double bottom simulating reflector in the eastern Nankai accretionary wedge: Results from full waveform inversion. Proc. of the 15th SEGJ Conf. The Society of Exploration Geophysicists of Japan, 2001. 90∼93

[30] Song H B, Matsubayashi O, Kuramoto S. Full waveform inversion of gas hydrate-related bottom simulating reflectors. *Chinese J. Geophys.* (in Chinese), 2003, **46**(1): 42∼46

[31] Wu Z Q, Chen J W, Gong J M. Genesis of BSR of gas hydrate in the sea areas. *Marine Geology Letter* (in Chinese), 2004, **20**(6): 25∼30

[32] Xu W, Ruppel C D. Predicting the occurrence, distribution and evolution of methane gas hydrate in porous marine sediments. *J. Geophys. Res.*, 1999, **104**: 5081∼5095

[33] Mienert J, Bryn P. Gas hydrate drilling conducted on the European margin. *EOS*, 1997, 567, 571

[34] Mienert J, Posewang J, Baumann M. Geophysical signature of gas hydrates along the north-eastern Atlantic Margins: Possible hydrate-bound margin instabilities and possible transfer of methane from oceanosphere to atmosphere. In: Henriet J P, Mienert J eds. Gas Hydrates: Relevance to World Margin Stability and Climate Change. Geological Society Special Publication, 1998, **137**: 275∼292

[35] Berndt C, Bunz S, Clayton T, et al. Seismic character of bottom simulating reflectors: examples from the mid-Norwegian margin. *Marine and Petroleum Geology*, 2004, **21**: 723∼733

[36] Foucher J P, Nouze H, Henry P. Observation and tentative interpretation of a double BSR on the Nankai slope. *Marine Geology*, 2002, **187**: 161∼175

[37] Nouze H, Noble M, Foucher J P, et al. Seismic imaging of a double BSR area on the Nankai slope. Proc. of 4th Inter. Conf. On Gas Hydrates, 2002. 158∼162

[38] Hovland M, Francis T J G, Claypool G E, et al. Strategy for scientific drilling of Marine gas hydrates. *JOIDES Journal*, 1999, **25**(1): 20∼24

[39] Zhang G X, Huang Y Y, Chen B Y. Seismology of Natural Gas Hydrate in the Sea (in Chinese). Beijing: Ocean Press, 2003

[40] Andreassen K, Hart P, Mackay M. Amplitude versus offset modeling of the bottom simulating reflection associated with submarine gas hydrates. *Marine Geology*, 1997, **137**: 25∼40

[41] Carccione J M, Tinivella U. Bottom simulating reflectors: seismic velocities and AVO effects. *Geophysics*, 2000, **65**: 54∼67

[42] Sun C Y, Zhang M Y, Niu B H, et al. Modeling of seismic blanking zone for gas hydrate. *Earth Science Frontiers* (in Chinese), 2003, **10**(1): 199∼204

[43] Sun C Y, Zhang M Y, Niu B H, et al. Study of modeling seismic bottom simulating reflector for natural gas hydrate. *Geoscience* (in Chinese), 2003, **17**(3): 337∼344

[44] Singh S C, Minshull T A, Spence G D. Velocity structure of a gas hydrate reflector. *Science*, 1993, **260**: 204∼207

[45] Singh S C, Minshull T A. Velocity structure of a gas hydrate reflector at Ocean Drilling Program site 889 from a global seismic waveform inversion. *J. Geophys. Res.*, 1994, **99**: 24221∼24233

[46] Minshull T A, Singh S C, Westbrook G K. Seismic velocity structure at a gas hydrate reflector, offshore western Colombia, from full waveform inversion. *J. Geophys. Res.*, 1994, **99**: 4715∼4734

[47] Yuan T, Spence G D, Hyndman R D, et al. Seismic velocity studies of a gas hydrate bottom simulating reflector on the northern Cascadia continental margin:Amplitude modeling and full waveform inversion. *J. Geophys. Res.*, 1999, **104**: 1179∼1191

[48] Keiiti Aki, Paul G Richards. Quantitative Seismology Theory and Methods, Vol.1. The Maple-Vail Book Manufacturing Group, USA. 1980

[49] Ruan A G, Li X Y. Analysis of AVA method for gas hydrate study. *Journal of Marine Sciences* (in Chinese), 2006, **24**(4): 22∼28